(Fig. 1). The difference between the SPICE and the TLM simulations during the transient period is due to the adaptive time-step used by SPICE. The frequency response in Fig. 1 Fig. 1(b) has been evaluated after the steady-state condition has been reached (t > 2.915 ns).

As a second example we have modeled the dynamic behavior of a pn-junction diode placed at one extremity of a stripline. The TLM analysis of the given structure has been compared with the results obtained using SPICE (Fig. 2Fig. 2), showing an excellent agreement both for the voltage and current behavior

Further details can be found in:

L. Cascio, G. Tardioli and W. J. R. Hoefer, "Modeling of Nonlinear Active and Passive Devices in Three-Dimensional TLM Networks", in IEEE Intl. Microwave Symp. Dig, pp. 383-386, Denver, Colorado, June 8-13, 1997.

2) Special 3D-TLM Corner Nodes for Singular Field Regions

(Giampaolo Tardioli, Lucia Cascio, Mario Righi, and Wolfgang J.R. Hoefer)

Introduction

Space discrete methods such as Finite Difference Frequency Domain (FDFD), Finite Difference Time Domain (FDTD), Transmission Line Matrix (TLM) and Finite Element Methods (FEM), are currently used for solving a wide variety of fields problems. The computational domain is discretized in a finite number of elementary cells where the electromagnetic field is assumed to have a simple behavior, very often linear. This assumption fails to accurately model sharp features, where highly nonuniform fields are present. This is typically the case of corners and edges, where the electromagnetic fields are singular. We refer to the resulting error as "coarseness error".

In time domain methods, a comparison between the dispersion and the coarseness error reveals that the coarseness error is the dominant source of inaccuracies in most of the practical cases and represents the most severe limitation to the maximum admissible cell size.

A direct solution to reduce the coarseness error is to use an extremely fine mesh, but this quickly leads to unacceptable memory and time requirements. A better approach is to use a variable or multigrid mesh, so that a higher resolution can be obtained in that region. In this case the resources would be still larger than those of a uniform coarser mesh fixed by the dispersion error only.

We present a novel approach to incorporate knowledge of the static field behavior in the vicinity of singularities in a three-dimensional TLM mesh. The procedure is systematic and does not require optimization of the correcting elements. As a result, relatively coarse TLM meshes may be used to obtain highly accurate results, within the dispersion error, across a wide frequency range.

Theoretical Background

Close to edges (Fig. 1) the spatial derivatives of the fields are much larger than the time derivatives, so that the latter may be neglected in Maxwell's equations. Therefore the propagation effects are negligible and the electromagnetic field is quasi-static. The finite energy condition imposes that the **E** and **H** field components normal to the corner become singular, while the **E** and **H** tangential components remain finite.

In particular, for a knife wedge (α=0), the y-field components can be expressed as:

$$E_y(r, \phi, t) = \alpha(t) r^{1/2} \sin\left(\frac{\phi}{2}\right) + \beta(t) \cdot r \cdot \sin(\phi) + \gamma(t) r^{3/2} \sin\left(\frac{3}{2}\phi\right) + \ldots \tag{1}$$

$$H_y(r, \phi, t) = c_0(t) + c_1(t) \cdot r^{1/2} \cdot \sin\left(\frac{\phi}{2}\right) + c_2(t) r \sin(\phi) + \ldots \tag{2}$$

Considering Maxwell's equations written in the cylindrical coordinate system y-r-ϕ, we obtain:

$$\frac{\partial H_r}{\partial y} - \frac{\partial H_y}{\partial r} = \varepsilon_0 \frac{\partial E_\phi}{\partial t} \qquad \frac{\partial E_r}{\partial y} - \frac{\partial E_y}{\partial r} = -\mu_0 \frac{\partial H_\phi}{\partial t} \tag{3}$$

where Ey and Hy in the vicinity of the corner are given by (1)(1), and (2)(2).

Edge Singularity, TM-Polarization

Consider the case of the knife edge embedded in a TLM mesh as depicted in Fig. 2.

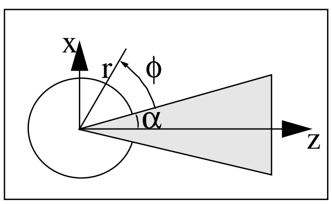

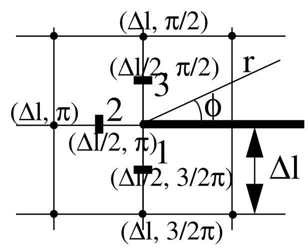

Fig. 1Perfectly conducting wedge	Fig. 2Knife edge in a TLM mesh; the edge is placed on TLM nodes

We want to implement the equations (3) including the edge condition (1) and (2) at the three TLM link lines. In particular for the TMy polarization (Hy=0), we have:

$$\mu_0 \left.\frac{\partial H_\phi\left(\frac{\Delta}{2}, \phi, t\right)}{\partial t}\right|_{\phi = \frac{\pi}{2}, \pi, \frac{3}{2}\pi} = \left.\frac{\partial E_y\left(\frac{\Delta}{2}, \phi, t\right)}{\partial r}\right|_{\phi = \frac{\pi}{2}, \pi, \frac{3}{2}\pi} - \left.\frac{\partial E_r\left(\frac{\Delta}{2}, \phi, t\right)}{\partial y}\right|_{\phi = \frac{\pi}{2}, \pi, \frac{3}{2}\pi} \tag{4}$$

Replacing the time derivative with the central difference scheme, recalling the mapping between voltages and fields between link lines in the 3D-SCN node, and using the static expansion in (2) we obtain the following modified scattering procedure for higher-order approximation:

$$G(\phi, k) = \frac{1}{2}\alpha(k\Delta t)\left(\frac{\Delta l}{2}\right)^{-\frac{1}{2}} \sin\left(\frac{\phi}{2}\right) + \beta(k\Delta t)\sin(\phi) + \frac{3}{2}\gamma(k\Delta t)\left(\frac{\Delta l}{2}\right)^{\frac{1}{2}} \sin\left(\frac{3}{2}\phi\right)$$

$$V_k^r = V_k^i + V_{k-1}^r - V_{k-1}^i + \frac{\Delta l^2}{2} \cdot \left(G(\phi, k) - \frac{\partial E_r}{\partial y}\right) \tag{5}$$

where Z0 is link line characteristic impedance, V_k^r are the voltage pulses incident on the points 1,2,3 from *the corner node* and V_k^i are the voltage pulses incident on the points 1,2,3 from *the external nodes* at the *kth* iteration.

The coefficients $\alpha(t)$, $\beta(t)$, $\gamma(t)$ are unknown. Their value can be determined by evaluating the electric field *Ey* at the three adjacent nodes at each time step and solving a linear system.

Similar calculations can be carried out for the TE polarization, obtained a modified scattering procedure similar to that depicted in the previous formula.

Results

In order to validate the proposed approach for the two different polarizations, we have implemented the algorithm in the 3D-SCN node, and computed the first resonant frequency of the cavities depicted in Fig. 3 and Fig. 4. The first structure is a rectangular cavity with an asymmetric inductive iris in the center.

Fig. 3Resonant cavity in rectangular waveguide with inductive coupling

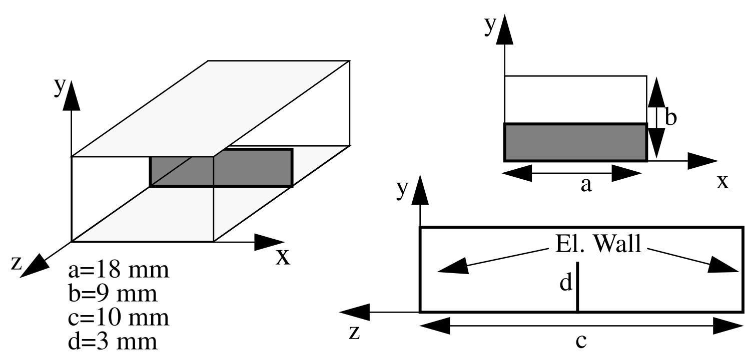

Fig. 4Resonant cavity in parallel plate waveguide with capacitive coupling

The second structure is a parallel plate waveguide resonator with an asymmetric capacitive iris in the middle. In both situations the new method as been compared with results available in the literature and with those obtained with the standard TLM algorithm with increasingly small discretization steps. Even with a very coarse mesh the introduction of the static-field correction yields an improvement in the accuracy with negligible impact on the computational time; the percentage error is reduced from 3.8% to 1% in the case of the TM polarization (Table 1), and from 10% to 0.3% in the case of TE polarization (Table 2). These results are consistent with those obtained with a standard TLM algorithm with cell sizes five to six times smaller with a significant saving in computational effort.

Table 1 Inductive Iris cavity resonant frequencies (GHz)

Δl	1 mm	1/3 mm	1/5 mm
TLM	31.732	31.062	30.922
Marcuvitz	30.560	-	-
Static Correction	30.889	-	-

Table 2 Capacitive Iris Cavity Resonant Frequencies (GHz)

Δl	1 mm	1/3 mm	1/5 mm	1/11 mm
TLM	11.175	11.935	12.105	12.260
Marcuvitz	12.475	-	-	-
Static Correction	12.510		-	-

Conclusion

A novel systematic procedure to incorporate static field configuration into a 3D-TLM mesh has been proposed. The method introduces the correct field singularity by exploiting the previous incident and reflected link-line voltages surrounding the corner node. The procedure requires negligible additional operations and leads to a saving in computational time and memory of two orders of magnitude.

Further details can be found in:

G. Tardioli, L. Cascio, and W. J. R. Hoefer, “Special 3D-TLM Corner Nodes for Singular Field Regions”, in 1997 IEEE MTT Symposium Dig., pp. 317-320, Denver, Colorado, June 9-13, 1997.

3) Characterization of Surface Mount Package Effects with the TLM Method

(Giampaolo Tardioli, Mario Righi, Lucia Cascio, and Wolfgang J. R. Hoefer)

Introduction

A typical problem facing designers of integrated circuits is to determine the effect of the package on the performance of a monolythic microwave integrated circuit (MMIC) it contains. The presence of leads, bond wires and grounding pins affects the MMIC behavior. These effects must be included in the early design stages. In order to avoid costly design cycles, an electromagnetic approach becomes attractive to predict accurately the performances of a packaged circuit.

We have performed the full wave time-domain analysis of a surface mount plastic package containing a simplified MMIC (a thru connection and a microstrip spiral inductor). Problems such as poor grounding terminations and crosstalk with neighboring lines are also considered as they can occur at relatively low frequencies.

Finally, we propose an approach to isolate the package effects. The whole structure is segmented and the package is characterized by its scattering parameters. In this way the package needs only to be modeled once for a given configuration. The package effects are extracted and combined with the MMIC parameters to predict the performance of the packaged circuit at a fraction of the computational costs. In addition, the MMIC circuit can be optimized by including the package effects from the design stages, thus signifi-